Proc. Natl. Acad. Sci. USA
Vol. 91, pp. 6240–6244, June 1994
Neurobiology

Primary structure and characterization of a small-conductance inwardly rectifying potassium channel from human hippocampus

FRANÇOIS PÉRIER, CAROLYN M. RADEKE, AND CAROL A. VANDENBERG

Department of Biological Sciences and Neuroscience Research Institute, University of California, Santa Barbara, CA 93106

Communicated by John Carbon, March 28, 1994 (received for review February 28, 1994)

ABSTRACT **We have isolated a human hippocampus cDNA that encodes an inwardly rectifying potassium channel, termed HIR (hippocampal inward rectifier), with strong rectification characteristics. Single-channel recordings indicate that the HIR channel has an unusually small conductance (13 pS), distinguishing HIR from other cloned inward rectifiers. RNA blot analyses show that HIR transcripts are present in heart, skeletal muscle, and several different brain regions, including the hippocampus.**

K^+ channels constitute a highly diverse group including voltage-gated and Ca^{2+}-activated channels belonging to the Shaker superfamily (1) and a distinct class of channels, the inward rectifiers. Inwardly rectifying K^+ channels are characterized by a decrease in K^+ conductance as the membrane potential becomes positive with respect to the K^+ equilibrium potential (E_K); as a result, these channels carry large inward currents and small outward currents (2).

The asymmetrical conductances of inward rectifiers are critical for the maintenance and modulation of cellular excitability. Inward rectifiers constitute the major class of K^+ channels in the heart, where they are involved in the onset and termination of the long-duration action potentials, in the regulation of heart-beat frequency, and in the determination of the resting potential (2–4). In the central nervous system, inwardly rectifying K^+ currents are present in neuronal and nonneuronal cells, including hippocampal neurons and astrocytes (5–8), and are thought to participate in electrical signaling and information processing.

In contrast to the fixed voltage-dependence of most ion channel mechanisms, the voltage-dependence of inward rectification varies with the external K^+ concentration ($[K^+]_o$), causing the voltage at which rectification occurs to shift in parallel with E_K. Open channel block by internal Mg^{2+} is the primary cause of both rapid inward rectification (9–11) and the dependence of rectification on external K^+ (9, 11, 12). Inwardly rectifying K^+ channels are multi-ion single-file pores, with multiple binding sites for both permeant and blocking ions (12). This characteristic is reflected by the approximate square-root dependence of their conductance on $[K^+]_o$ (12).

The primary structures of three inwardly rectifying K^+ channels, ROMK1, IRK1, and GIRK1/KGA have been reported recently (13–16). These inward rectifiers show homologies with K^+ channels of the Shaker superfamily in the H5 domain, thought to be the central core of the channel pore (13, 14), but are markedly different in other regions. In addition, only two putative membrane-spanning domains bracket the H5 region of inward rectifier polypeptides, in contrast to the six transmembrane domains of Shaker-type K^+ channels.

We have cloned a cDNA encoding a human inwardly rectifying K^+ channel, HIR (hippocampal inward rectifier), present in brain and muscle tissues.* We have expressed the HIR channel in *Xenopus* oocytes, and we have shown that it is a classical strong inward rectifier, displaying large inward currents and minimal outward currents. The amino acid sequence of HIR has homology to those of other inward rectifiers but contains significant differences, indicating that HIR is a previously unreported member of the inward rectifier family. Electrophysiological analyses of this channel demonstrate that HIR represents a class of inwardly rectifying K^+ channels characterized by a small unitary conductance.

MATERIALS AND METHODS

Isolation of HIR cDNA Clones. Two oligonucleotides of sequences corresponding to base pairs (bp) 7–26 and 333–352 of cDNA clone HHCMD37 (17) were 3′-end-radiolabeled and used in combination to screen 2×10^5 independent plaques from a human hippocampal Lambda ZAP II cDNA library (Stratagene) by plaque hybridization (18). Another 5×10^5 plaques were screened by using a third probe (5′-TGGGAAGACGCAGGGCCAAG-3′) whose sequence was derived from the 5′-end of the largest cDNA clone obtained in the first screen. Positive candidates were further screened by excising and rescuing the respective plasmids (18) and analyzing their cDNA inserts by restriction mapping and sequencing.

DNA Sequencing and Sequence Analyses. Both strands of the HIR cDNA were sequenced from single-stranded templates by using Sequenase (United States Biochemical), primers evenly spaced at ≈200-bp intervals, and both dGTP and dITP in parallel reactions. GELASSEMBLE, PEPPLOT, and GAP from the Genetics Computer Group package were used for sequence assembly, analysis, and alignment, respectively.

***In Vitro* Transcription and Oocyte Preparations.** HIR cDNA was transcribed *in vitro* by using T3 RNA polymerase and G(5′)ppp(5′)G (18). IRK1 cRNA was synthesized in a similar manner. *Xenopus laevis* oocytes were injected with ≈50 nl of HIR complementary RNA (cRNA) at 6 ng/μl or IRK1 cRNA at 10 ng/μl for two-electrode voltage-clamp recordings or HIR cRNA at 30 ng/μl for cell-attached patch-clamp recordings (19, 20).

Two-Microelectrode Voltage-Clamp Recordings. Oocyte currents were recorded as described (19, 20). The standard recording solution (96 mM K^+) contained 91 mM KCl, 5 mM $MgCl_2$, 10 mM Hepes (5 mM KOH to pH 7.5), and 0.15 mM each of niflumic and flufenamic acids. $BaCl_2$ and CsCl were added to the 96 mM K^+ solution without compensating for the change in ionic strength. Recordings were performed at 23–24°C. The fractional electrical distance δ for the Cs^+ binding site within the membrane electric field was calculated according to Woodhull (21).

Cell-Attached Patch-Clamp Recordings. Single-channel recordings were performed from cell-attached patches using a

The publication costs of this article were defrayed in part by page charge payment. This article must therefore be hereby marked "*advertisement*" in accordance with 18 U.S.C. §1734 solely to indicate this fact.

Abbreviations: E_K, potassium equilibrium potential; $[K^+]_o$, external potassium ion concentration; HIR, hippocampal inward rectifier; cRNA, complementary RNA.

*The sequence reported in this paper has been deposited in the GenBank data base (accession no. U07364).

Dagan 3900 integrating patch clamp (Dagan Instruments, Minneapolis) interfaced with an Axolab data acquisition system (Axon Instruments, Foster City, CA) and an 80386-based computer for voltage-pulse generation and acquisition (22). Both pipette and bath solutions contained 150 mM KCl, 2 mM $MgCl_2$, 1 mM EGTA, and 10 mM Hepes, adjusted to pH 7.2 with KOH. Recordings were performed at room temperature (≈22°C).

RNA Blot (Northern) Analyses. Human multiple tissue and human brain Northern blots (Clontech) were probed with the 1.9-kb HIR cDNA labeled with ^{32}P by random priming and with a ^{32}P-labeled human β-actin cDNA (18). Final washes prior to autoradiography were at 50°C in 0.015 M NaCl/ 0.0015 M sodium citrate/0.1% SDS.

RESULTS

Molecular Cloning of HIR. We identified in the GenBank data base a 392-bp DNA sequence whose deduced amino acid sequence in one reading frame had significant homologies with a 130-amino acid region of inwardly rectifying channels ROMK1, IRK1, and GIRK1/KGA, including part of the H5 and M2 domains. This expression sequence tag had been obtained originally from a cDNA clone (HHCMD37) isolated from a human hippocampus cDNA library (17) and represented the full-length of the clone. We postulated that HHCMD37 was a partial copy of a mRNA coding for a polypeptide homologous to inward rectifiers that we named HIR. Using probes derived from the HHCMD37 DNA sequence, we isolated three positive clones from a human hippocampus cDNA library. The 1.9-kb cDNA insert of one clone had a poly(A) tail located at one end and contained a region nearly identical to the reported 392-bp sequence of clone HHCMD37; the other candidates had shorter 5′ sequences. None of the inserts of nine positive clones obtained through a second screen with a probe derived from the sequence of the 5′ end of the 1.9-kb cDNA extended further upstream.

Primary Structure of HIR. The sequence of the 1.9-kb HIR cDNA clone contains an open reading frame of 1335 nucleotides coding for a 445-amino acid polypeptide (Fig. 1). The presumed translation initiation ATG codon is preceded 21 nucleotides upstream by a TGA stop codon in the same reading frame, indicating that this 1.9-kb cDNA sequence contains the entire coding sequence. Hydrophobicity analysis of the HIR polypeptide indicates the presence of two transmembrane domains, termed M1 and M2 in Fig. 1. Several potential phosphorylation sites are present in the primary sequence of HIR (Fig. 1 legend).

The deduced amino acid sequence of HIR has 44%, 67%, and 44% identity with aligned ROMK1, IRK1, and GIRK1/ KGA sequences, respectively (Fig. 2). Regions of HIR displaying high homology with these other inward rectifiers include the M1, M2, and putative pore (H5) domains. Several regions of marked divergence are apparent in Fig. 2. Most notably, a 21-amino acid stretch of small neutral amino acids (residues 91–111) is present in HIR but absent in ROMK1, IRK1, and GIRK1/KGA. The 60-amino acid N-terminal domain of HIR is shorter than that of the other inward rectifiers (82–86 amino acids), and the first 19-amino acid residues of this domain show only weak sequence homology with the corresponding residues of these other inward rectifiers. Similarly, the C-terminal 56-amino acid sequence of HIR displays weak homology with the carboxyl end of the three other inwardly rectifying channels.

Functional Expression of HIR. *Xenopus* oocytes injected with HIR cRNA expressed K^+-selective currents with strong inward rectification (Fig. 3 *a* and *b*). Large inward currents were elicited by voltage steps negative to E_K, and little or no current was elicited by more positive voltages. These currents had a peak amplitude of 16 ± 7 μA (mean ± SD; n = 22) at −170 mV in the 96 mM K^+ bath solution, were blocked by 3 mM external Ba^{2+} (Fig. 4*e*), were insensitive to 100 μM tolbutamide in the external bath, and were absent in control water-injected oocytes (data not shown).

K^+ Selectivity of HIR. The HIR current was K^+-selective; substitution of external K^+ with Na^+ was accompanied by a decrease in Ba^{2+}-sensitive currents (Fig. 3*a*). A slow voltage-dependent Na^+ block was apparent when NaCl was substituted for KCl in the bath solution. The reversal potential of HIR currents followed E_K (Fig. 3 *b* and *c*). A 10-fold change in $[K^+]_o$ led to a 64 ± 5 mV (mean ± SD; n = 3) change in reversal potential, in agreement with the change in E_K predicted by the Nernst equation (59 mV).

```
 -97  GAGAATTTCAACCAGAAAGAACAGCCAGTGCAAAGGCCCAGAGACAGGAATAAACTTGGCCCTGCGTCTTCCCAGGTGACCACGCCGGCTTCAGGAC  -1
   1  ATGCACGGACACAGCCGCAACGGCCAGGCCCACGTGCCCCGGCGGAAGCGCCGCAACCGCTTCGTCAAGAAGAACGGCCAATGCAACGTGTACTTCGCCAACCTGAGCAACAAGTCGCAG  120
   1  M  H  G  H  S  R  N  G  Q  A  H  V  P  R  R  K  R  R  N  R  F  V  K  K  N  G  Q  C  N  V  Y  F  A  N  L  S  N  K  S  Q  40
                                                                                          M1
 121  CGCTACATGGCGGACATCTTCACCACCTGCGTGGACACGCGCTGGCGCTACATGCTCATGATCTTCTCCGCGGCCTTCCTTGTCTCCTGGCTCTTTTTCGGCCTCCTCTTCTGGTGTATC  240
  41  R  Y  M  A  D  I  F  T  T  C  V  D  T  R  W  R  Y  M  L  M  I  F  S  A  A  F  L  V  S  W  L  F  F  G  L  L  F  W  C  I  80
 241  GCCTTCTTCCACGGTGACCTGGAGGCCAGCCCAGGGGTGCCTGCGGCGGGGGGCCCGGCGGCGGGTGGTGGCGGAGCAGCCCCGGTGGCCCCCAAGCCCTGCATCATGCACGTGAACGGC  360
  81  A  F  F  H  G  D  L  E  A  S  P  G  V  P  A  A  G  G  P  A  A  G  G  G  G  A  A  P  V  A  P  K  P  C  I  M  H  V  N  G  120
                                  H5                                                                 M2
 361  TTCCTGGGTGCCTTCCTGTTCTCGGTGGAGACGCAGACGACCATCGGCTATGGGTTCCGGTGCGTGACAGAGGAGTGCCCGCTGGCAGTCATCGCTGTGGTGGTCCAGTCCATCGTGGGC  480
 121  F  L  G  A  F  L  F  S  V  E  T  Q  T  T  I  G  Y  G  F  R  C  V  T  E  E  C  P  L  A  V  I  A  V  V  V  Q  S  I  V  G  160
 481  TGCGTCATCGACTCCTTCATGATTGGCACCATCATGGCCAAGATGGCGCGGCCCAAGAAGCGGGCGCAGACGTTGCTGTTCAGCCACCACGCGGTCATTTCGGTGCGCGACGGCAAGCTC  600
 161  C  V  I  D  S  F  M  I  G  T  I  M  A  K  M  A  R  P  K  K  R  A  Q  T  L  L  F  S  H  H  A  V  I  S  V  R  D  G  K  L  200
 601  TGCCTCATGTGGCGCGTGGGCAACCTGCGCAAGAGCCACATTGTGGAGGCCCACGTGCGGGCCCAGCTCATCAAGCCCTACATGACCCAGGAGGGCGAGTACCTGCCCCTGGACCAGCGG  720
 201  C  L  M  W  R  V  G  N  L  R  K  S  H  I  V  E  A  H  V  R  A  Q  L  I  K  P  Y  M  T  Q  E  G  E  Y  L  P  L  D  Q  R  240
 721  GACCTCAACGTGGGCTATGACATCGGCCTGGACCGCATCTTCCTGGTGTCGCCCATCATCATTGTCCACGAGATCGACGAGGACAGCCCGCTTTATGGCATGGGCAAGGAGGAGCTGGAG  840
 241  D  L  N  V  G  Y  D  I  G  L  D  R  I  F  L  V  S  P  I  I  I  V  H  E  I  D  E  D  S  P  L  Y  G  M  G  K  E  E  L  E  280
 841  TCGGAGGACTTTGAGATCGTGGTCATCCTGGAGGGCATGGTGGAGGCCACGGCCATGACCACCCAGGCCCGCAGCTCCTACCTGGCCAGCGAGATCCTGTGGGGCCACCGCTTTGAGCCT  960
 281  S  E  D  F  E  I  V  V  I  L  E  G  M  V  E  A  T  A  M  T  T  Q  A  R  S  S  Y  L  A  S  E  I  L  W  G  H  R  F  E  P  320
 961  GTGGTCTTCGAGGAGAAGAGCCACTACAAGGTGGACTACTCACGTTTTCACAAGACCTACGAGGTGGCCGGCACGCCCTGCTGCTCGGCCCGGGAGCTGCAGGAGAGTAAGATCACCGTG  1080
 321  V  V  F  E  E  K  S  H  Y  K  V  D  Y  S  R  F  H  K  T  Y  E  V  A  G  T  P  C  C  S  A  R  E  L  Q  E  S  K  I  T  V  360
1081  CTGCCCGCCCCACCGCCCCCTCCCAGTGCCTTCTGCTACGAGAACGAGCTGGCCCTTATGAGCCAGGAGGAAGAGGAGATGGAGGAGGAGGCAGCTGCGGCGGCCGCGGTGGCCGCAGGC  1200
 361  L  P  A  P  P  P  P  P  S  A  F  C  Y  E  N  E  L  A  L  M  S  Q  E  E  E  E  M  E  E  E  A  A  A  A  A  A  V  A  A  G  400
1201  CTGGGCCTGGAGGCGGGTTCCAAGGAGGAGGCGGGCATCATCCGGATGCTGGAGTTCGGCAGCCACCTGGACCTGGAGCGCATGCAGGCTTCCCTCCCGCTGGACAACATCTCCTACCGC  1320
 401  L  G  L  E  A  G  S  K  E  E  A  G  I  I  R  M  L  E  F  G  S  H  L  D  L  E  R  M  Q  A  S  L  P  L  D  N  I  S  Y  R  440
1321  AGGGAGTCTGCCATCTGACCTCCAGGCCCGGCCCTCACCACTGCCCACAAGAGCCTCTGCCGGGGGTGGGATGCCAGGACACCCCCTCCCACACTCAGGACAGAGCCAACCCTGGCTCCG  1440
 441  R  E  S  A  I  *                                                                                                       445
1441  TGGACCTTCTGGAGGAAGGTGGGGGTTTCAAAGACTGGGGGACCCCTTCCTCCTGACTCCAGCACCCAGGCCTGGGAAGAGCTCGGCCCCGATCAGCCTGAGTTCCGCCAGCGCCTACTT  1560
1561  CTGGTGGCTCTAGGTCCCCGGATCCACCACCCTTCCCCCACTGACTCTTCAAGGACGTGCCCTCTTTGCTCTCAGAACCTTGGGGAAGGTGGCTGGACTGCTGGGCGGGGGACATCTCGG  1680
1681  GGTTTCAGGGTGGGCAGGGGGTTAGTTTGGGGAGGGGGGGGTGCGTTTCTTTTGCATGACTGTGGCCTGTTGCTCATGACTTTCTTTTGTAAATATCTATAAATGGAGACAGATGGAGAC  1800
1801  ACCAAAAAAAAAAAAAA                                                                                                       1816
```

FIG. 1. Nucleotide and deduced amino sequence in single-letter code of HIR cDNA. The in-frame TGA stop codon of the 5′ untranslated region is underlined. Putative transmembrane (M1 and M2) and pore (H5) domains are indicated. Potential phosphorylation sites include Tyr-234 and Tyr-333, within consensus epidermal growth factor receptor kinase phosphorylation site sequences; Ser-212, Ser-306, and Ser-443, within consensus cAMP-dependent kinase phosphorylation site sequences; and Ser-36, Ser-39, Thr-143, Ser-194, Ser-212, Ser-306, Ser-349, Thr-359, Ser-438, and Ser-443, within consensus protein kinase C phosphorylation site sequences.

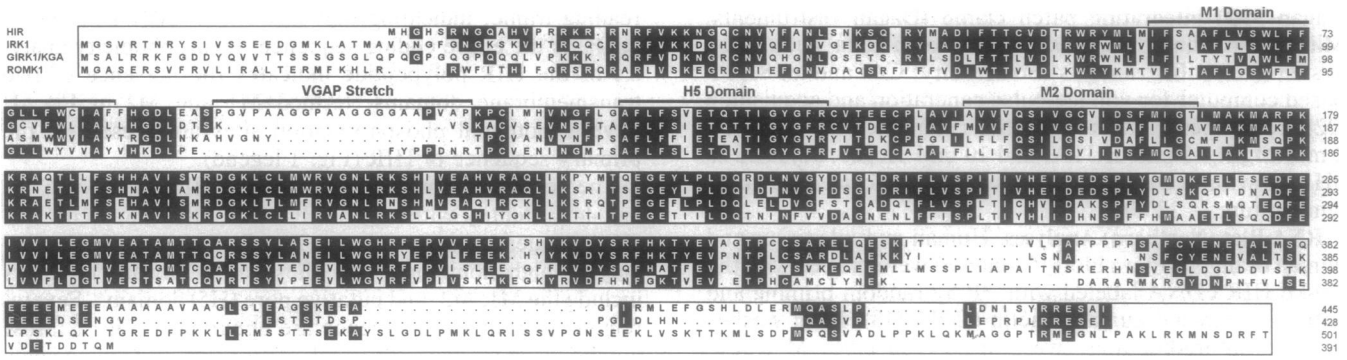

FIG. 2. Amino acid sequence (single-letter code) comparison between HIR, IRK1 (14), GIRK1/KGA (15, 16), and ROMK1 (13). Alignments were optimized by introducing gaps. Black boxes indicate amino acid identities between HIR and the other inward rectifiers. VGAP, Val-Gly-Ala-Pro.

Dependence of HIR Rectification on $[K^+]_o$. The voltage at which rectification takes place varies as the external K^+ concentration is changed and follows E_K (Fig. 3*b*), as expected for a typical inward rectifier (11, 23–25).

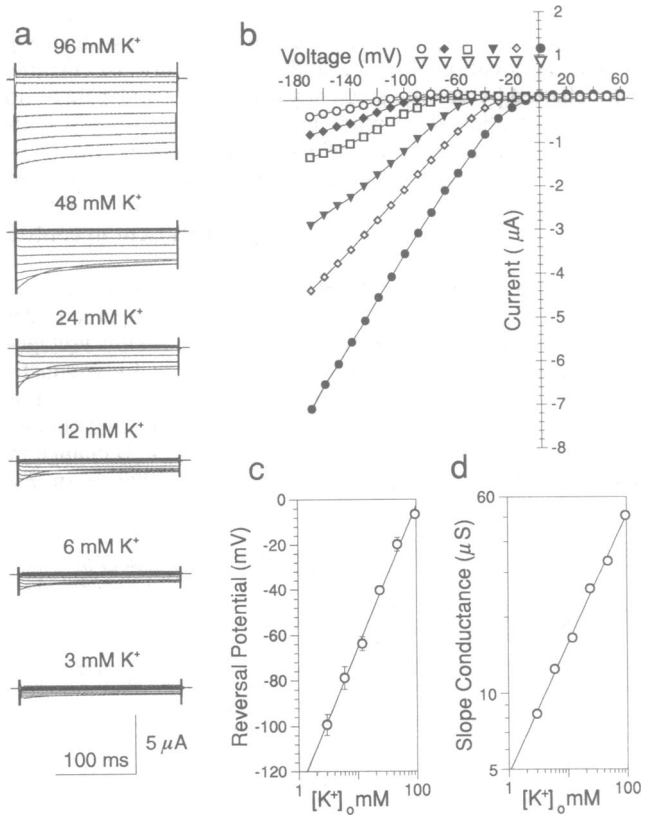

FIG. 3. Electrophysiological characterization of HIR. (*a*) Currents were recorded from a HIR cRNA-injected oocyte voltage-clamped at −20 mV and subjected to 200-ms voltage pulses from −170 to +60 mV in 10-mV increments. Current traces obtained every 20-mV are shown. Currents were recorded in external solutions of various K^+ concentrations as indicated, with substitution of Na^+ for K^+. Records were filtered at 5 kHz. (*b*) Ba^{2+}-sensitive peak currents from *a* are plotted as a function of applied voltage. Data points represent the peak currents minus currents recorded in the presence of 3 mM Ba^{2+}. Predicted E_K values are indicated by the open arrows below the corresponding symbol. $[K^+]_o$: ●, 96 mM; ◇, 48 mM; ▼, 24 mM; □, 12 mM; ◆, 6 mM; and ○, 3 mM. (*c*) Reversal potential of Ba^{2+}-sensitive HIR currents vs. $[K^+]_o$ (mean ± SD; n = 3). Data were fitted by linear regression. (*d*) HIR conductance vs. $[K^+]_o$. Slope conductances were measured between −140 and −120 mV from the *I–V* plot in *b*. Data were fitted with the following equation: conductance = $A([K^+]_o)^x$, giving a value for x of 0.5.

Dependence of HIR Conductance on $[K^+]_o$. A double-logarithmic plot of the HIR slope conductance as a function of $[K^+]_o$ is linear, with a slope of ≈0.5 (n = 3), indicating a

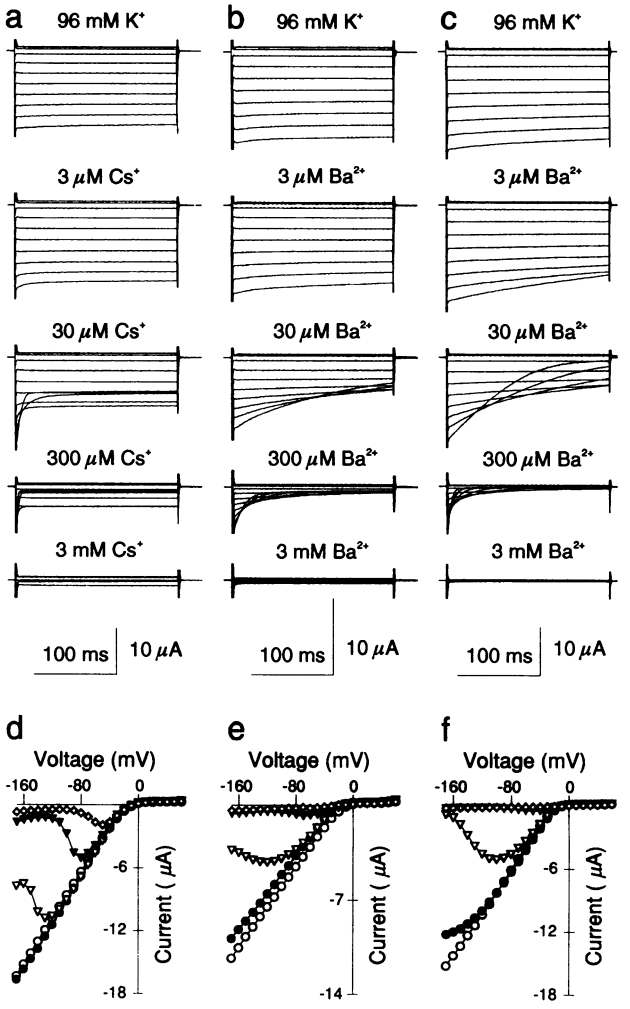

FIG. 4. Cs^+ and Ba^{2+} block of HIR and IRK1 currents. (*a–c*) Currents were recorded from either HIR or IRK1 cRNA-injected oocytes as in Fig. 3. Oocytes were bathed in external solutions containing 96 mM K^+ and increasing concentrations of Cs^+ or Ba^{2+} as indicated. (*a*) Block of HIR by Cs^+. (*b*) Block of HIR by Ba^{2+}. (*c*) Block of IRK1 by Ba^{2+}. (*d–f*) *I–V* plots from *a–c* for the block of HIR currents by Cs^+ (*d*) and Ba^{2+} (*e*) and for the block of IRK1 currents by Ba^{2+} (*f*). Currents were measured at the end of the 200-ms test pulses. External blocking ion concentrations were 0 μM (○), 3 μM (●), 30 μM (▽), 300 μM (▼), and 3 mM (◇).

square-root dependence of HIR conductance on $[K^+]_o$ (Fig. 3*d*). As for other inward rectifiers, this indicates that the pore of HIR is simultaneously occupied by multiple K^+ ions (12, 24, 25).

External Block of HIR by Cs^+ and Ba^{2+}. Extracellular Cs^+ and Ba^{2+} were potent and specific blockers of HIR currents and interacted with the channel in a time-, voltage-, and concentration-dependent manner (Fig. 4 *a*, *b*, *d*, and *e*) as described for other inward rectifiers (23–27). By measuring steady-state currents in the absence and presence of Cs^+ (Fig. 4 *a* and *d*), we calculated a theoretical fractional electrical distance (δ) of 1.4 ± 0.2 (mean ± SD; $n = 6$) for the Cs^+ binding site within the membrane electric field. This value is similar to the fractional distance of 1.53 reported for the voltage-dependent block of IRK1 by Cs^+ ions (14) and indicates multiple occupancies. Increasing concentrations of $BaCl_2$ in the bath solution also resulted in a time- and voltage-dependent block of HIR currents (Fig. 4 *b* and *e*). Comparison of current profiles in the presence of different concentrations of Ba^{2+} in the external solution showed that HIR (Fig. 4 *b* and *e*) is less sensitive to Ba^{2+} block than IRK1 (Fig. 4 *c* and *f*). This difference was apparent in all HIR cRNA-injected ($n = 15$) and IRK1 cRNA-injected ($n = 6$) oocytes tested for Ba^{2+} block in parallel experiments. Because of slow kinetics, we did not quantitate the Ba^{2+} block of HIR and IRK1 channels (Fig. 4 *e* and *f*).

Cell-Attached Single-Channel Profile of HIR. Single HIR channels carried inward K^+ currents at membrane voltages negative to E_K and minimal outward current at potentials above E_K (Fig. 5*a*). As noted for many other strongly inwardly rectifying K^+ channels, HIR gating kinetics were slow, with long open times at negative potentials and a reduction in channel open time at very negative potentials (14, 24, 25, 28–32).

Voltage steps between negative potentials at which the HIR channel was open and equivalent positive potentials showed that rectification of HIR currents was almost instantaneous (Fig. 5*b*): Open HIR channels exhibited a rapid change in conductance as the membrane potential was changed from negative to positive values. The single-channel conductance of HIR with a 150 mM K^+ pipette solution was 13 ± 1 pS (mean ± SD; $n = 3$; Fig. 5*c*), significantly less than the 21–42 pS conductances reported for other cloned inwardly rectifying potassium channels under similar conditions (13–16).

Tissue Distribution of HIR mRNA. A multiple-tissue Northern blot of human poly(A)$^+$ RNA was probed with the ^{32}P-labeled 1.9-kb HIR cDNA. (Fig. 6 *Left*). The HIR probe hybridized strongly to a mRNA species of ≈2.7-kb present in heart and brain tissues. In addition, a 5-kb message showed homology to HIR sequences in skeletal muscle. Since the HIR cDNA was originally isolated from a hippocampal cDNA library, we analyzed the distribution of HIR mRNA in distinct anatomical regions of the brain (Fig. 6 *Right*). The 2.7-kb HIR transcript was particularly abundant in three telencephalic structures, the amygdala, caudate nucleus, and hippocampus, and, to a lesser extent, in the thalamus. In contrast, a slightly larger mRNA species (≈3 kb) hybridizing to the HIR probe was most abundant in the corpus callosum, hypothalamus, substantia nigra, and subthalamic nucleus. The sequence of the 3-kb message is distinct from HIR cDNA, since more extensive washes specifically reduced the 3-kb signal intensity (data not shown).

DISCUSSION

We have identified a previously unreported inwardly rectifying potassium channel, HIR. This channel displays all the characteristics of classical inward rectifiers with strong rectification properties and a unique feature, low single-channel conductance.

Primary structure data show that HIR has homologies with inward rectifiers ROMK1, IRK1, and GIRK1/KGA, with conserved putative transmembrane and pore domains (13–16). A unique stretch of small neutral amino acids, termed the "VGAP" (Val-Gly-Ala-Pro) stretch, is present in HIR between the first transmembrane domain (M1) and the H5 region (Fig. 2). The VGAP stretch significantly extends the length of the M1-to-H5 linker, thought to lie on the extracellular side of the membrane, and may have a functional role in the conductance or permeation properties of HIR. The N and C termini of HIR are also distinct from those of ROMK1, IRK1, and GIRK1/KGA. These end domains diverge most among these other inward rectifiers as well and are likely to participate in the unique gating and modulation characteristics of the channels. Searches of current data bases did not reveal significant homologies between the unique regions of HIR and other known proteins.

Among inward rectifiers, IRK1 shows the highest degree of amino acid sequence identity with HIR. This sequence similarity is reflected in the electrophysiological properties of

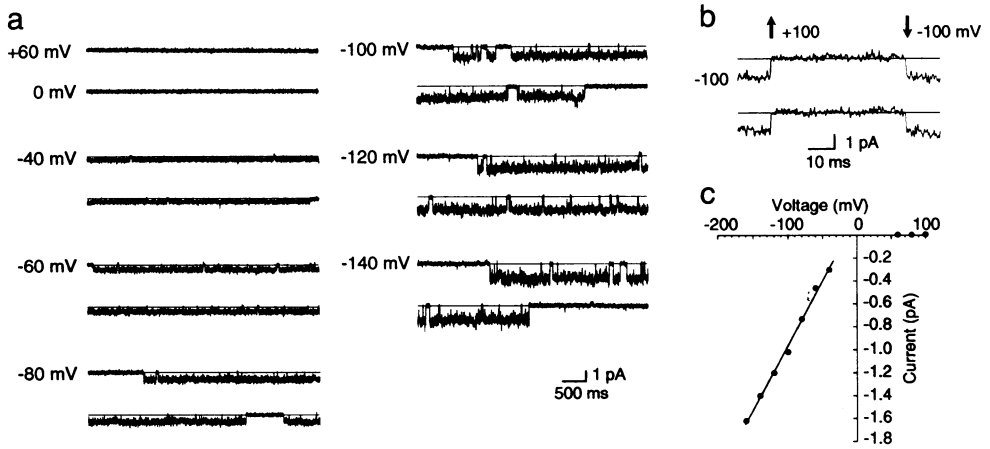

FIG. 5. Cell-attached single-channel recordings of HIR currents. (*a*) Continuous single-channel current recordings are shown from a patch held at the indicated potentials. (*b*) Instantaneous rectification of single-channel HIR currents. Current traces from a single open HIR channel held at −100 mV and subjected to a 50-ms pulse to +100 mV are shown. Arrows indicate the start and the end of the depolarizing pulse. Linear leakage and capacitative currents were subtracted by using averaged blank records. All currents were filtered at 1 kHz. (*c*) *I–V* relationship of a single HIR channel from *a*.

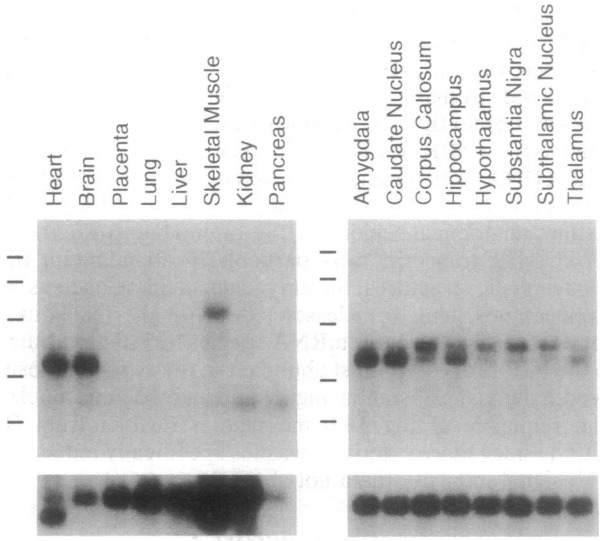

FIG. 6. Tissue distribution of HIR mRNA. (*Upper Left*) Northern analysis of human poly(A)$^+$ RNA from various tissues probed with the ^{32}P-labeled 1.9-kb HIR cDNA. (*Lower Left*) The same blot was probed with ^{32}P-labeled human β-actin cDNA for comparison and shows hybridization to both 2-kb and muscle-specific 1.7-kb messages. (*Right*) Northern blot of human poly(A)$^+$ RNA from anatomical brain subregions probed with the ^{32}P-labeled 1.9-kb HIR cDNA (*Upper Right*) and with ^{32}P-labeled human β-actin cDNA (*Lower Right*). The position of RNA size markers (from top to bottom: 9.5 kb, 7.5 kb, 4.4 kb, 2.4 kb, and 1.35 kb) is indicated on the left.

these two channels, since their currents rectify strongly near E_K and they both display slow single-channel gating kinetics. In contrast, ROMK1 currents exhibit moderate rectification, and GIRK1/KGA single channels have faster gating kinetics (13–16). HIR and IRK1 are clearly distinct channels, however; their single-channel conductances markedly differ (13 pS for HIR and 21 pS for IRK1), and they have different sensitivities to external Ba^{2+} block. Furthermore, HIR and the highly conserved human homolog of IRK1 are encoded by distinct size classes of mRNA that do not cross-hybridize (K. Raab and C.A.V., unpublished data).

HIR probes detect a 2.7-kb mRNA species in heart and brain tissues and a 5-kb transcript in skeletal muscle (Fig. 6). The 2.7-kb HIR mRNA is most abundant in specific neuronal regions, and a slightly larger transcript with weaker homology to HIR sequences is detectable in other brain regions. This prominent distribution in the central nervous system shows that HIR rectifiers represent an important class of brain K$^+$ channels. The tissue distribution of HIR transcripts overlaps with that reported for IRK1- and GIRK1/KGA-related messages (13–16). This mRNA colocalization parallels the observation that single cells can display both small- and large-conductance inwardly rectifying K$^+$ channels (29–32). Developmental regulation or formation of heteromultimeric inward rectifiers may provide additional functional diversity (30, 32).

Single-channel recordings show that HIR exhibits the smallest single-channel conductance (13 ± 1 pS) of the cloned inward rectifiers. Inwardly rectifying K$^+$ channels with similar unitary conductances to that of HIR have been described in skeletal muscle cells (28, 29), in cardiac ventricular myocytes (24, 30, 32), and in cerebral capillary endothelial cells (31). These inward rectifiers are identical to HIR in terms of strong inward rectification characteristics and long single-channel open times. We propose that both HIR and IRK1 channels contribute to the strongly rectifying K$^+$ currents of these cells and participate in establishing action potential waveform and excitability of neuronal and muscle tissues.

Until now, the identification of small-conductance inwardly rectifying K$^+$ channels has been obscured by the inherent small amplitudes of their currents and by the frequent open sublevels of high-conductance channels (24, 25). The molecular cloning of HIR described in this report will allow both molecular dissection of a novel channel and electrophysiological characterization of a small-conductance inward rectifier.

We thank L. Y. Jan for providing the IRK1 cDNA clone, K. Coulter and K. Raab for sharing unpublished results and reagents, and E. Choi and M. Radeke for helpful discussions. This work was supported by grants from the National Institutes of Health (HL41656), the American Heart Association, California Affiliate, and by a National Multiple Sclerosis postdoctoral fellowship (to F.P.).

1. Strong, M., Chandy, K. G. & Gutman, G. A. (1993) *Mol. Biol. Evol.* **10**, 221–242.
2. Vandenberg, C. A. (1993) in *Ion Channels in the Cardiovascular System: Function and Dysfunction*, eds. Brown, A. M., Catterall, W. A., Kaczorowski, G. J., Spooner, P. M. & Strauss, H. C. (Futura, Mount Kisco, NY), in press.
3. Noma, A. (1987) in *Electrophysiology of Single Cardiac Cells*, eds. Noble, D. & Powell, T. (Academic, London), pp. 223–246.
4. Shimoni, Y., Clark, R. B. & Giles, W. R. (1992) *J. Physiol. (London)* **448**, 709–727.
5. Yamaguchi, K., Nakajima, Y., Nakajima, S. & Stanfield, P. R. (1990) *J. Physiol. (London)* **426**, 499–520.
6. Brown, D. A., Gahwiler, B. H., Griffith, W. H. & Halliwell, J. V. (1990) *Prog. Brain Res.* **83**, 141–160.
7. Wimpey, T. L. & Chavkin, C. (1991) *Neuron* **6**, 281–289.
8. Tse, F. W., Fraser, D. D., Duffy, S. & MacVicar, B. A. (1992) *J. Neurosci.* **12**, 1781–1788.
9. Horie, M. & Irisawa, H. (1987) *Am. J. Physiol.* **253**, H210–H214.
10. Matsuda, H., Saigusa, A. & Irisawa, H. (1987) *Nature (London)* **436**, 156–159.
11. Vandenberg, C. A. (1987) *Proc. Natl. Acad. Sci. USA* **84**, 2560–2564.
12. Hille, B. & Schwarz, W. (1978) *J. Gen. Physiol.* **72**, 409–442.
13. Ho, K., Nichols, C. G., Lederer, W. J., Lytton, J., Vassilev, P. M., Kanazirska, M. V. & Hebert, S. C. (1993) *Nature (London)* **362**, 31–38.
14. Kubo, Y., Baldwin, T. J., Jan, Y. N. & Jan, L. Y. (1993) *Nature (London)* **362**, 127–133.
15. Kubo, Y., Reuveny, E., Slesinger, P. A., Jan, Y. N. & Jan, L. Y. (1993) *Nature (London)* **364**, 802–806.
16. Dascal, N., Schreibmayer, W., Lim, N. F., Wang, W., Chavkin, C., DiMagno, L., Labarca, C., Kieffer, B. L., Gaveriaux-Ruff, C., Trollinger, D., Lester, H. A. & Davidson, N. (1993) *Proc. Natl. Acad. Sci. USA* **90**, 10235–10239.
17. Adams, M. D., Dubnick, M., Kerlavage, A. R., Moreno, R., Kelley, J. M., Utterback, T. R., Nagle, J. W., Fields, C. & Venter, J. C. (1992) *Nature (London)* **355**, 632–634.
18. Sambrook, J., Fritsch, E. F. & Maniatis, T. (1989) *Molecular Cloning: A Laboratory Manual* (Cold Spring Harbor Lab. Press, Plainview, NY).
19. Périer, F., Coulter, K. L., Radeke, C. M. & Vandenberg, C. A. (1992) *J. Neurochem.* **59**, 1971–1974.
20. Stuhmer, W. (1992) *Methods Enzymol.* **207**, 319–339.
21. Woodhull, A. M. (1973) *J. Gen. Physiol.* **61**, 687–708.
22. Hamill, O. P., Marty, A., Neher, E., Sakmann, B. & Sigworth, F. J. (1981) *Pflügers Arch.* **391**, 85–100.
23. Hagiwara, S., Miyazaki, S. & Rosenthal, N. P. (1976) *J. Gen. Physiol.* **67**, 621–638.
24. Kameyama, M., Kiyosue, T. & Soejima, M. (1983) *Jpn. J. Physiol.* **33**, 1039–1056.
25. Sakmann, B. & Trube, G. (1984) *J. Physiol. (London)* **347**, 641–657.
26. Standen, N. B. & Stanfield, P. R. (1978) *J. Physiol. (London)* **280**, 169–191.
27. DiFrancesco, D., Ferroni, A. & Viscentin, S. (1984) *Pflügers Arch.* **402**, 446–453.
28. Ohmori, H., Yoshida, S. & Hagiwara, S. (1981) *Proc. Natl. Acad. Sci. USA* **78**, 4960–4964.
29. Matsuda, H. & Stanfield, P. R. (1989) *J. Physiol. (London)* **414**, 111–124.
30. Josephson, I. R. & Sperelakis, N. (1990) *Biochim. Biophys. Acta* **1052**, 123–127.
31. Hoyer, J., Popp, R., Meyer, J., Galla, H. & Gogelein, H. (1991) *J. Membr. Biol.* **123**, 55–62.
32. Masuda, H. & Sperelakis, N. (1993) *Am. J. Physiol.* **265**, H1107–H1111.